Mausam, (1991), **42**, 3, 241-248

551.511.13 : 551.513.5

A model study of the 30-50 day oscillation in the tropical atmosphere

S. V. KASTURE, V. SATYAN and R.N. KESHAVAMURTY
Physical Research Laboratory, Navrangpura, Ahmedabad
(Received 27 June 1990)

सार — सी.आई.एस.के. (CISK) तरंग निर्माण के साथ भूमंडलीय मानावलीय निदर्श का प्रयोग करते हुए हमने पूर्व की ओर गतिमान भूमध्य रेखीय प्रणाली बनाई है जो कि 30-50 दिन की प्रेक्षित प्रणाली के समान लगती है। इसके ऊर्ध्वाधर में भूमंडलीय तरंग संख्या एक और दो परत की संरचना वाला मापक होता है। इसकी संरचना में केल्विन तथा रोसबी तरंगे मिश्रित होती हैं। यह मिश्रित प्रणाली पूर्व की ओर चलती है।

अरैखिक मानावलीय निदर्श की अनुक्रिया को समझने के लिए हमने द्वि-स्तरीय रैखिक विश्लेषणात्मक निदर्श का भी अध्ययन किया है। रैखिक निदर्श तथा अरैखिक मानावलीय निदर्श में भी जब हम आर्द्रता उपलब्धता कारक को बढ़ाते हैं तो सभी तरंगों की गति घटती है। रैखिक निदर्श में यह गति सभी प्रकार की तरंगों के लिए कर्षण से मुक्त पाई गई है। अरैखिक मानावलीय निदर्श में दिए गए एक कर्षण में आर्द्रता उपलब्धता कारक का क्रांतिक मान होता है, जिसके लिए तरंग स्थिर हो जाती है और इसके बाद भी पश्चिम की ओर संचरण करती दिखाई देती है। इस प्रकार आर्द्रता उपलब्धता तथा अरैखिकता दोनों ही भूमध्य रेखीय की 30-50 दिन की प्रणाली की पूर्व की ओर की गति को धीमी करने में योगदान देने लगते हैं।

ABSTRACT. Using a global spectral model with wave-CISK formulation we have generated an eastward moving equatorial mode which resembles the observed 30-50 day mode. This has a scale of global wave number one and a two layer structure in the vertical. It has the structure of a composite of Kelvin and Rossby waves. This composite system moves eastwards.

We have also studied a linear two-level analytical model to understand the nonlinear spectral model response. In the linear model as well as in the nonlinear spectral model, as we increase the moisture availability factor the speeds of all the waves decrease. In the linear model this speed is found to be independent of drag for all types of waves. In the nonlinear spectral model for a given drag there is a critical value of the moisture availability factor for which the wave becomes stationary and beyond which even shows westward propagation. Thus both moisture availability and nonlinearity appear to contribute to the slow eastward speed of the equatorial 30-50 day mode.

Key words — 30-50 day oscillation, wave-CISK, moisture availability factor, moist Kelvin wave, Rossby wave, primitive equation global spectral model, analytical two-level model.

1. Introduction

One of the important quasi-regular features in the tropical atmosphere on the sub-seasonal time scale is the 30-50 day oscillation. This oscillation was first found in the equatorial region by Madden and Julian (1971). The oscillation consisted of east-west circulation in the longitude-height plane and had a slow eastward movement. Dakshinamurti and Keshavamurty (1976) found large power in the 30-day time scale in their power spectrum analysis of zonal component of wind in the Indian monsoon region. Alexander *et al.* (1978) composited wind and contour height data of active and break phases over India and found a slow northward movement. Analysis of satellite cloudiness data by Yasunari (1979, 1980) and Sikka & Gadgil (1980) reveal slow northward movement of cloud bands on this time scale. Krishnamurti and Subrahmanyam (1982) found a northward propagating mode in the zonal winds in the Indian region. Studies by Krishnamurti *et al.* (1985) showed a 30-50 day oscillation in the 200 mb divergent component of wind and the mode showed eastward propagation and had a dominant scale of wave number one. Lorenc (1984) using FGGE data found an eastward propagating wave-number-one mode on this time scale. Murakami *et al.* (1983) found the structure of this oscillation using FGGE data. The global nature of this oscillation was revealed by studies of radiation and wind data by Weickmann *et al.* (1975). Knutson *et al.* (1980) and Lau and Chan (1983 a & b, 1985, 1986). Kasture and Keshavamurty (1987) studied the structure and period of this oscillation and also found some interannual variability in it. Keshavamurty *et al.* (1986) found low frequency oscillation generated by an equatorial heat source when the model outputs were low pass filtered. They also used a zonally symmetric two-level model and found that meridional propagation in the monsoon region was possible. On the theoretical front several studies have been carried

out to understand the origin and movement of 30-50 day oscillation. A complete understanding is yet to emerge. Lau and Peng (1987) have proposed a theory of this low frequency oscillation. Using a linear model they found that a slow eastward propagation of an equatorial disturbance occurs using mobile wave-CISK formulation. In the present study we have used their wave-CISK formulation in a nonlinear global spectral model and generated such a slow eastward propagating mode. Using a linear/nonlinear model Hendon (1988) studied the influence of moisture availability and drag on the equatorial mode. Chao (1987) in his linear study showed that the speed of this mode is related to the vertical heating profile and it decreases with dissipation and the zonal size of the convective region. Chang and Lim (1988) showed that there is interaction of vertical modes and hence the low frequency mode has slow propagating speed. Most of the above models were linear models. Hendon used a two-level model in which the momentum equations were linear and the thermodynamic energy equation was nonlinear. He concentrated only the first baroclinic mode. The barotropic mode was not present. In our present study we use a fully nonlinear 5-level global spectral model where both baroclinic and barotropic modes are present. We also scan a wider range of moisture availability factor (m) and drag. To obtain some physical insight we have also conducted linear model calculations.

2. Model study

2.1. *Slow eastward moving equatorial mode*

In our study we have used a five-level global spectral model based on the spectral model formulation as in Bourke (1974). The model has rhomboidal truncation at 10 waves and uses semi-implicit time integration scheme with a time step of one hour. We also have ∇^2 diffusion and a linear drag with a decay time of 5 days. The vertical levels in the model are shown below :

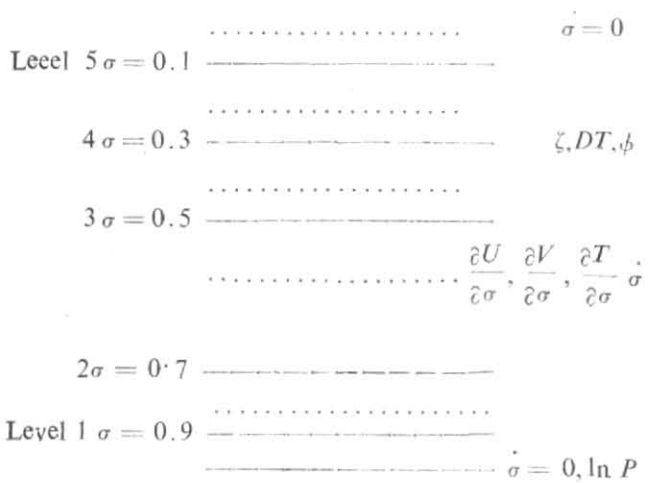

The studies have been conducted using a prescribed heating distribution. We started with a heating of 4°C per day in an area covered by 45° of longitude and 3.4°S to 3.4°N Gaussian latitudes. Thus, the heating distribution is symmetric with respect to the equator. The vertical profile of heating used is based on the study of Mohanty and Das (1986) which shows the maximum of cumulus heating at 500 mb. Therefore, a vertical distribution of heating of the form $\sin(\pi\sigma)$

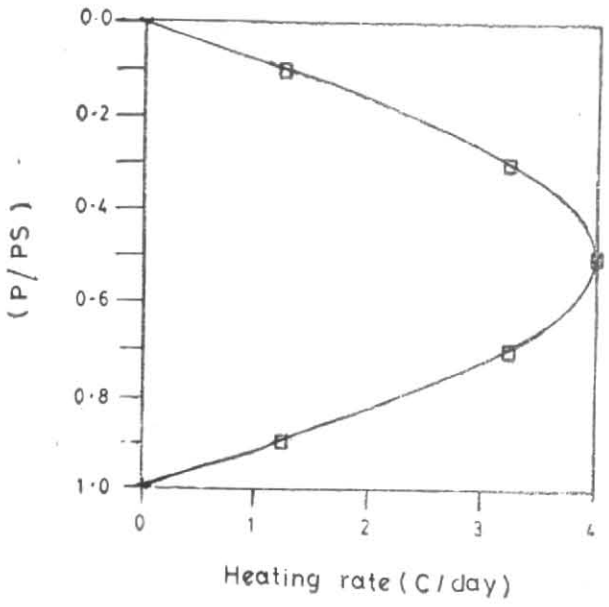

Fig. 1.

(Fig. 1) was chosen. The model was integrated with this equatorial heating for 5 days and then the heating was switched off. The purpose of this equatorial heating is to generate equatorial waves. Next wave-CISK heating as formulated in Lau and Peng (1987) was switched on. In this formulation the heating rate $\dot{Q}(\sigma)$ at level σ is given by :

$$\dot{Q}(\sigma) = \begin{cases} -m\,\eta(\sigma)\,r\,L\,q_{sat}(T_1)\,D_1\,\Delta\sigma/c_p & D_1 < 0 \\ 0 & D_1 \geq 0 \end{cases}$$

where, η — Normalised vertical profile of heating,

r — Relative humidity (0.75),

$q_{sat}(T_1)$ — Saturation specific humidity at temperature T_1 at the lowest model level,

D_1 — Divergence at the lowest level

m — Moisture availability factor,

L — Latent heat of condensation.

This type of heating (positive only) is proportional to the low level convergence. In the main experiment the model was integrated for 35 days with this wave-CISK heating with $m = 0.8$.

2.2. *Results and discussion*

Figs. 2 (a & b) show the time-longitude section of velocity potential in the equatorial region (3.4°N) at 300 and 900 mb. We see a marked eastward propagation with a period of 25 days. The wave has a horizontal scale of wave number one. The waves at 900 and 300 mb have a phase difference of 180°. Thus the wave has a two-layer structure with opposite phases in the upper and lower tropospheres.

Fig. 3(a) shows the time-longitude section of the zonal component of wind in the equatorial region at 300 mb and shows the eastward propagating mode with wave-number one scale, period of 25 days. The u-field in the lower troposphere (not shown) is similar to the

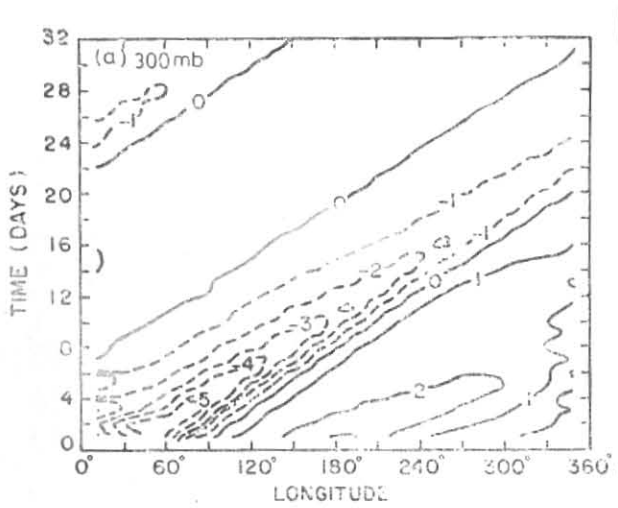

Fig. 2(a). Velocity potential (10^6 m^2 sec^{-1}) at 300 mb

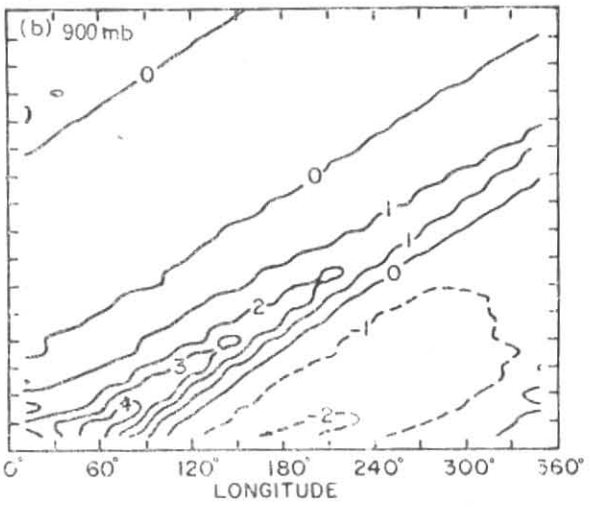

Fig. 2 (b). Velocity potential (10^6 m^2 sec^{-1}) at 900 mb

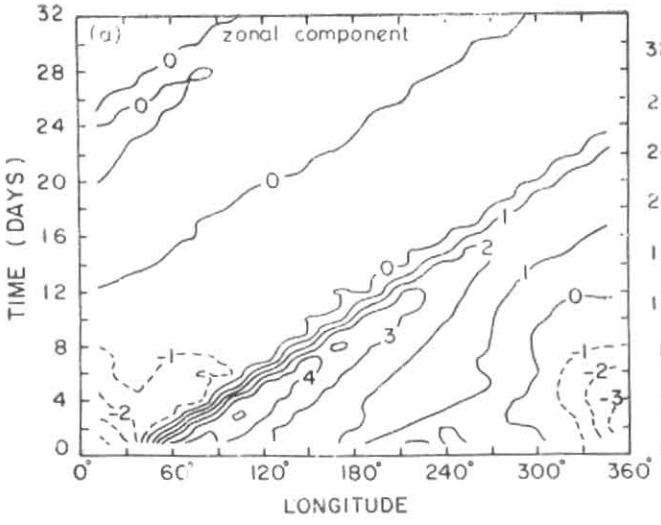

Fig. 3 (a). Zonal component of wind (m sec^{-1}) at 300 mb

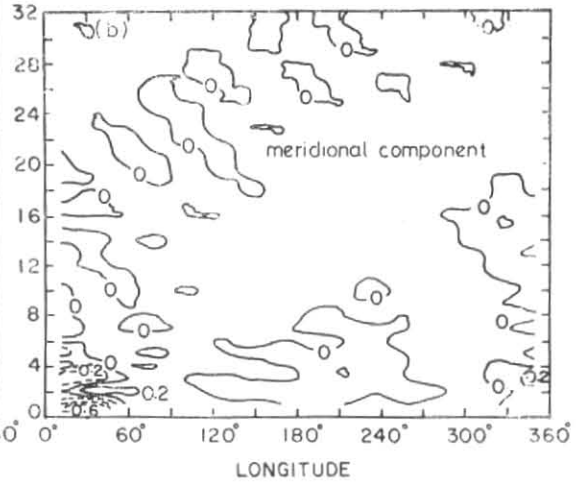

Fig. 3 (b). Meridional component of wind (m sec^{-1}) at 300 mb

field at 300 mb but has opposite phase. The same coherent oscillation is also seen at surface pressure and 300 mb and 900 mb in other fields such as temperature, stream function, vorticity and divergence. However, such an eastward propagating mode is not seen in the meridional component of wind either at 300 mb [Fig. 3(b)] or at 900 mb (Figure not shown). Thus the eastward propagating mode has the appearance of a moist Kelvin wave which feeds on the release of latent heat in clouds. The speed and scale are determined by equatorial atmospheric dynamics. The vertical structure is possibly determined by the vertical structure of the heating imposed initially which generated these waves.

The horizontal structure of these waves is better brought out in maps at 300 mb. Figs. 4(a-c) show the field of zonal component of wind at 300 mb on day 10, 20 and 30 respectively, clearly bringing out the eastward propagating mode. This takes about 25-30 days to go round the globe. The u-field is equatorially confined and has wave number one structure. Fig. 5 shows the u component at 900 mb on day 10. Comparing this with Fig. 4(a) we see that the two fields are of opposite phase bringing out the equatorial vertical circulations in the longitude height plane. From the horizontal structure maps it is difficult to conclude that the eastward moving mode is a pure Kelvin wave. The mode appears to be a composite of a Kelvin wave to the east and Rossby wave to the west. The composite wave moves eastwards.

Figs. 6 and 7 show the fields of velocity potential and temperature at 300 mb on day 10. The velocity potential field shows a simple wave number one structure. The temperature (Fig. 7) and zonal wind field [Fig. 4(a)] are more equatorially confined and all fields show symmetry about the equator. Thus, we have generated an equatorial 30-day oscillation starting from an equatorial heat source which has a vertical profile with a maximum at 500 mb. In a dry model with such a heat source Keshavamurty *et al.* (1986) obtained only a fast moving equatorial Kelvin wave of period 9 days. Only when the fields were low pass filtered low frequency oscillations were obtained. In out study we have introduced wave-CISK formulation of Lau and Peng (1987) and we get low frequency equatorial oscillation with a period of 25 days, wave number one scale and a two layer structure in the vertical.

The interesting feature is that we have generated this oscillation in a purely atmospheric model which has no land-ocean contrast, hydrology, cloud radiation feedback and such sophistications.

2.3. *Further studies with different moisture availability factors and drag*

We have conducted further studies to understand the role of m, the moisture availability factor and the drag. First we kept the linear drag constant at 15 days and varied m. We used steady equatorial heating for 15 days. Then the heating was switched off and wave-CISK was switched on. We conducted four runs with m=0.4, 0.6, 0.7 and 0.8. The model equations were integrated in each case for about 40 days. Figs. 8 (a-d) show the time longitude plots of the zonal component of wind (u) at 300 mb for the four cases of m. We notice steady eastward propagation in the first three cases. The period (time required to go round the globe once in the equatorial wave guide) increases from 16 days to 25 days as we increase m from 0.4 to 0.7. Thus, the eastward speed steadily decreases as we increase m. This is in general conformity with Hendon's (1988) results. However, for m=0.8 the moist Kelvin wave moves eastward for some time and then becomes stationary and grows in amplitude. This result is somewhat different from that of Hendon (1988), wherein he gets only eastward moving wave of 35-day period for some time and it dies down later on.

Next we study the effect of drag. We keep the moisture availability factor m=0.8 and vary the drag. Consider the Figs. 3(a), 9 and 8(d) for drag values of 5-day,

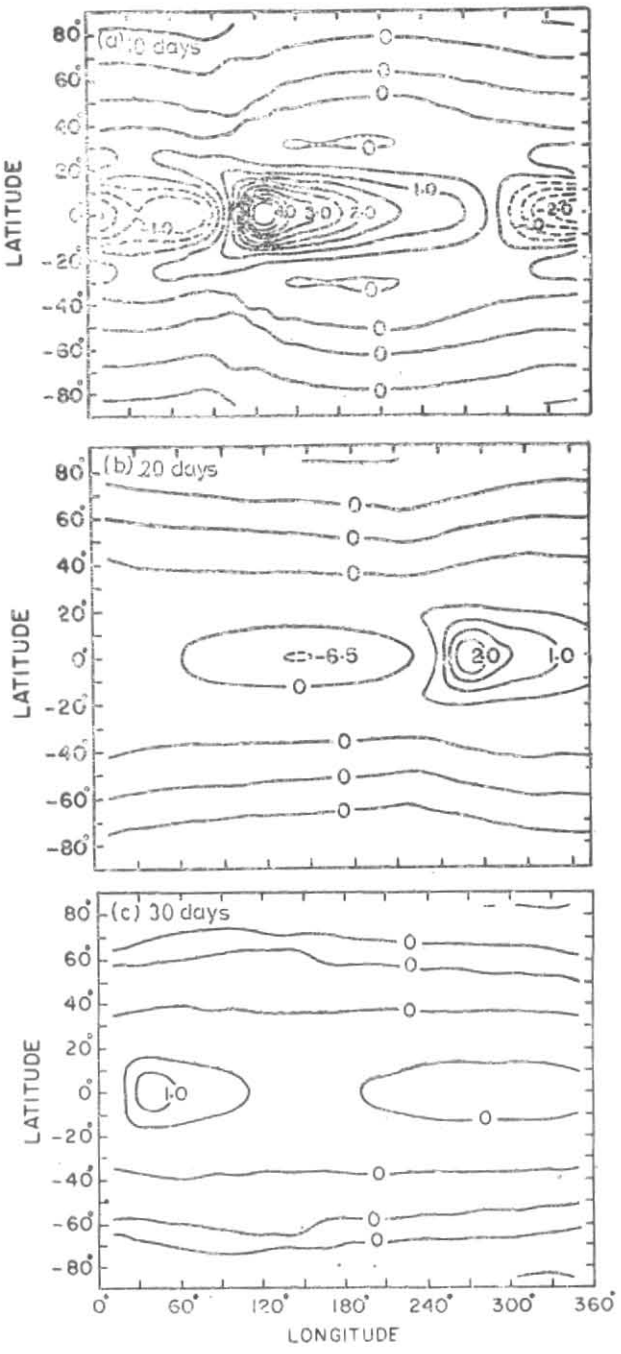

Figs. 4. (a-c). Zonal component of wind (m sec^{-1}) at 300 mb : (a) 10 days, (b) 20 days and (c) 30 days

10-day and 15-day respectively. It is clear that with less drag the eastward moving wave decreases in intensity more slowly. The more interesting result, however, is that, whereas for 5 and 10-day drags we get eastward moving wave, for 15-day drag this wave becomes stationary after some time.

We have also studied whether the critical moisture availability factor for which the eastward moving wave becomes stationary is different for different drags. Fig. 10 show the time-longitude plot of zonal compo-

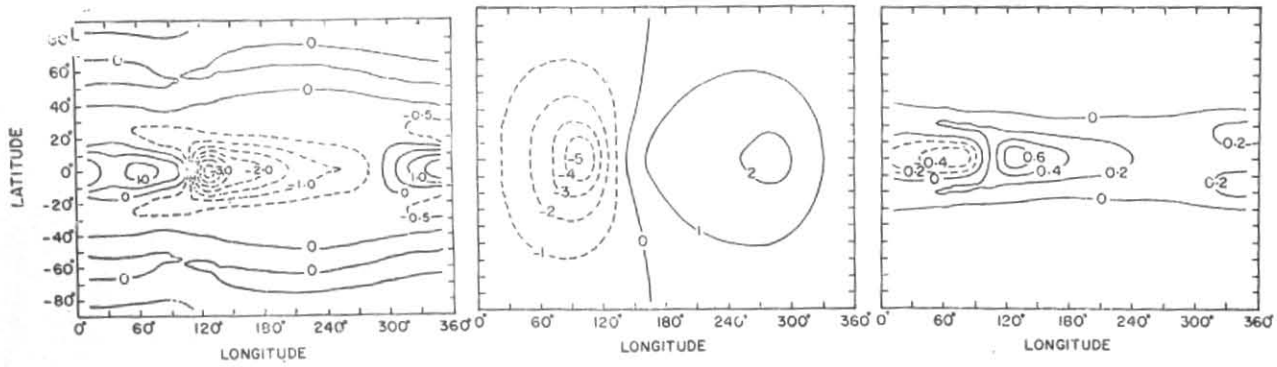

Fig. 5. Zonal component of wind at 900 mb, 10 days (m sec^{-1})

Fig. 6. Velocity potential at 300 mb, 10 days (10^6 m^2 sec^{-1})

Fig. 7. Temp. (°K) at 300 mb, 10 days

nent of wind at 300 mb for m=0.98 and a drag of 5 days. It is seen that initially the wave moves east and then starts moving westwards. However, we have seen earlier that for 15-day drag the wave becomes stationary for m=0.8. Thus, the critical m for the wave to become stationary or to start moving westwards appears to depend upon the drag. Hendon (1988) using a two level spectral model obtained an eastward moving wave with period around 90 days when he used m=0.98 and a drag of 5 days. He obtained a westward moving wave of 10-day period for m=1.15 and a drag of 15 days. These differences in the parameters for which the wave becomes stationary or moves westwards are possibly due to model differences. Ours is a 5-level model and is fully nonlinear.

2.4. *Linear model studies*

In order to gain some physical insight into the above model results, the low frequency variability is studied using an analytical model. We use a linear model on an equatorial β-plane and include linear drag and cumulus heating terms. The relevant equations for the perturbed quantities are

$$\frac{\partial u}{\partial t} - \beta y v = -\frac{\partial \phi}{\partial x} - k'' u \qquad (1)$$

$$\frac{\partial v}{\partial t} + \beta y u = -\frac{\partial \phi}{\partial y} - k'' v \qquad (2)$$

$$\frac{\partial}{\partial t}\left(\frac{\partial \phi}{\partial p}\right) + \sigma \omega = H - k'' \frac{\partial \phi}{\partial p} \qquad (3)$$

where the symbols have their usual meanings. σ is the static stability and k'' is the drag coefficient. The first term on the right hand side of the thermodynamic equation is cumulus heating. We use the wave-CISK cumulus heating parameterization of Lau and Peng (1987):

$$H = k'\left(\frac{\partial u}{\partial x} + \frac{\partial v}{\partial y}\right)$$

where, $k' = m\,R\,r\,L\,q_{sat}\,\eta(p)\,\triangle p/C_p p$,

m — Moisture availability factor,

R — Gas constant,

r — Relative humidity, set at 0.75,

L — Latent heat of condensation,

q_{sat} — Saturation specific humidity at the lowest model level,

$\eta(p)$ — Normalized vertical profile of heating,

C_p — Specific heat at constant pressure p.

The model has two levels :

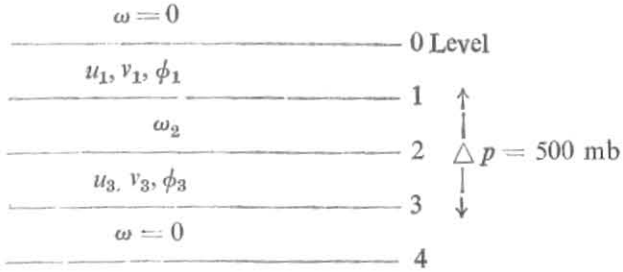

Using the continuity equation at levels 1 and 3 and the thermodynamic equation at level 2 we get :

$$\frac{\partial}{\partial t}\left(\frac{\hat{\phi}}{\triangle p}\right) + \omega_2\left(\frac{\sigma \triangle p - k'}{\triangle p}\right) = 0 \qquad (4)$$

where $\hat{\phi} = \phi_3 - \phi_1$

Eqns. (1), (2) and (4) are our model equations. Assuming their solutions in the form:

$$\left.\begin{matrix} u = \\ v = \\ \phi = \end{matrix}\right\} \begin{matrix} u(y) \\ v(y) \\ \phi(y) \end{matrix} \Bigg\} \; e^{i(kx + \lambda t)} \qquad (5)$$

we get

$$\frac{\partial^2 v}{\partial y^2} + \left(\frac{ik\beta}{D} - k^2 - \frac{2D^2}{\triangle p(\sigma \triangle p - k')} - \frac{2\beta^2 y^2}{\triangle p(\sigma \triangle p - k')}\right) v = 0 \qquad (6)$$

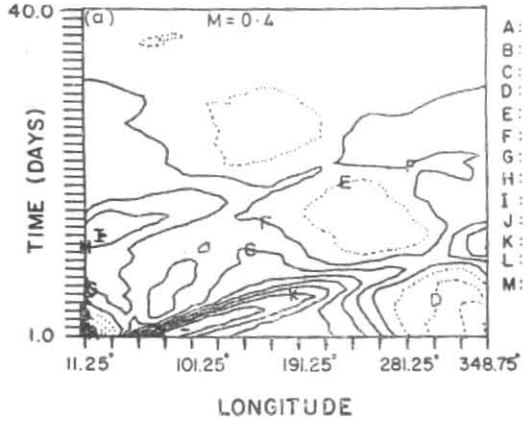

Fig. 8 (a). Zonal wind at 300 mb (drag 15 days) $m=0.4$

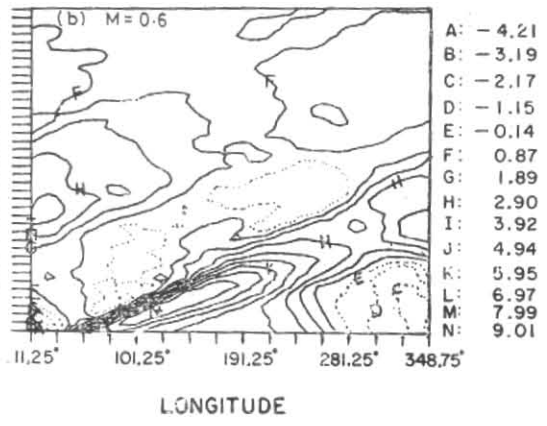

Fig. 8 (b). Zonal wind at 300 mb (drag 15 days) $m=0.6$

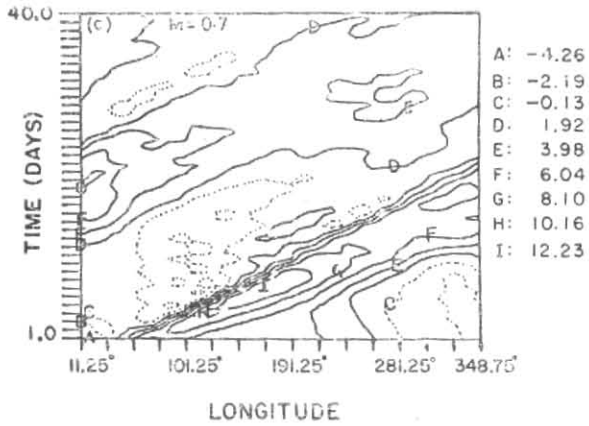

Fig. 8 (c). Zonal wind at 300 mb (drag 15 days) $m=0.7$

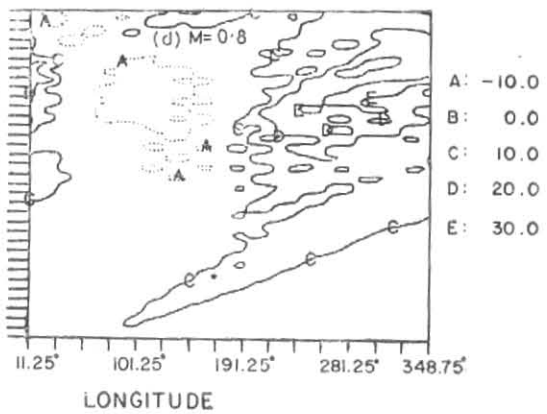

Fig. 8(d). Zonal wind at 300 mb (drag 15 days) $m=0.8$

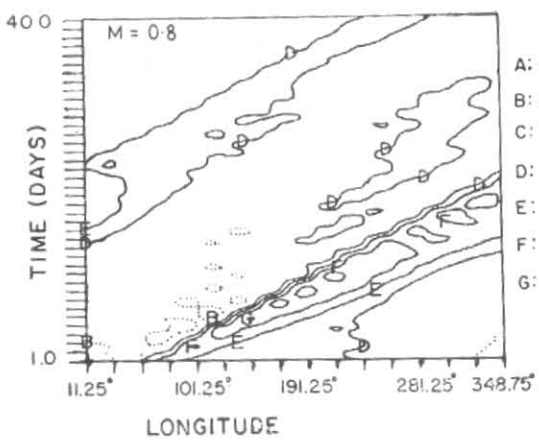

Fig. 9. Zonal wind at 300 mb (drag 10 days) $m=0.8$

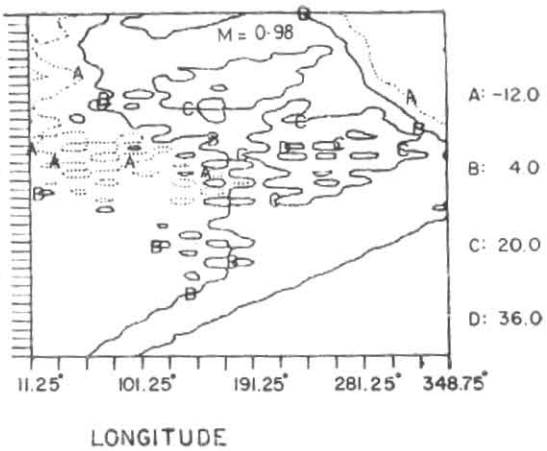

Fig. 10. Zonal wind at 300 mb (drag 5 days) $m=0.98$

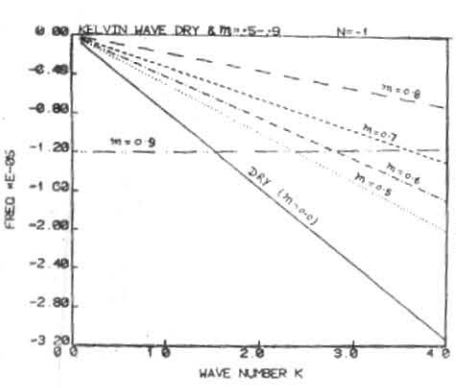

Fig. 11.

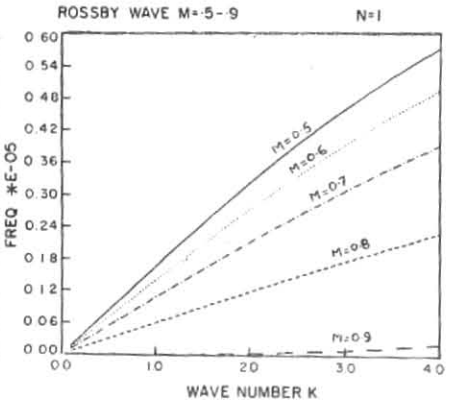

Fig. 12.

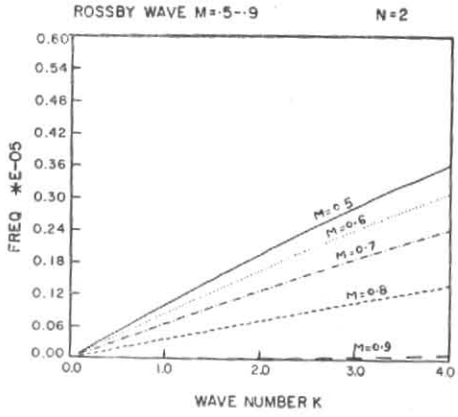

Fig. 13

where, $D = i\lambda + k''$. Since we are considering wave motions near the equator, the boundary conditions

$$v \to 0 \text{ as } y \to \pm \infty \qquad (7)$$

may be adequate. This boundary condition (7) is satisfied when the following relation is satisfied :

$$\frac{ik\beta}{D} - k^2 - \frac{2D^2}{\triangle p\,(\sigma \triangle p - k')} = (2n+1)\sqrt{\frac{2}{\triangle p\,(\sigma \triangle p - k')}}\,\beta \qquad (n = 0, 1, 2 \ldots\ldots) \qquad (8)$$

Eqn. (6) with boundary condition (7) poses an eigenvalue problem.

The solution of (6) is given as:

$$v(y) = C \exp(-1/2\,\beta A y^2)\, H_n(\beta A y) \qquad (9)$$

where, $A = \sqrt{\frac{2}{\triangle p\,(\sigma \triangle p - k')}}$, H_n is the Hermite polynomial of the n^{th} order and C is a constant.

Substituting $D = i\lambda + k''$ in Eqn. (8) and simplifying we get:

$$\lambda^3 - 3ik''\lambda^2 - \left(\frac{k^2}{A^2} + \frac{(2n+1)\beta}{A} + 3k''^2\right)\lambda + \frac{\beta k}{A^2} + \frac{i(2n+1)\beta}{A}k'' + ik''^3 + ik''k^2 = 0 \qquad (10)$$

For $n = -1$ Eqn. (10) has two solutions one of which does not satisfy the boundary condition. The other solution represents an equatorial Kelvin wave.

If $k'' = 0$ and $k' = 0$, Eqn. (10) gives solution for the dry Kelvin wave. We get the speed of this eastward propagating Kelvin wave as 50 ms^{-1} (Period 10 days) (see Fig. 11, $m = 0$). The speed of the waves is independent of drag. For different moisture availability factors m (0.5 to 0.9) the phase speed of the Kelvin wave is calculated and shown in Fig. 11 and Table 1. It is seen that in this linear analytical study also the period increases (phase speed decreases) as the moisture availability factor is increased. It is also seen that the speeds in the nonlinear model are slower. For $m = 0.9$, $k' > \sigma \triangle p$ and hence A is imaginary. The roots of Eqn. (10) give imaginary phase speed, *i.e.*, waves are stationary and they grow.

TABLE 1

Model/m	0.4	0.5	0.6	0.7	0.8	0.9	0.98
Linear model	—	15	18	23	41	Stationary	
Nonlinear model (Drag 15 days)	16	—	20	25	Stationary	—	
Nonlinear model (Drag 10 days)	—	—	—	—	25	—	—
Nonlinear model (Drag 5 days)	—	—	—	—	25	—	Westward

Variation of the period (in days) with moisture availability factor (m) and drag coefficient in different models.

Thus the speed of the moist Kelvin wave decreases as the moisture increases and beyond a certain m the wave becomes stationary and grows in amplitude.

We next examined this effect of increasing m (from 0.5 to 0.9) on the westward propagating Rossby waves (Figs. 12 and 13). The speed of the Rossby waves also decreases as m is increased from 0.5 to 0.8 and for $m = 0.9$ the waves become stationary.

We also find that the westward moving inertia gravity waves are slowed down more than the eastward moving inertia gravity waves as m, the moisture availability factor is increased.

3. Main results and conclusions

(*i*) Using a global spectral model and the wave-CISK cumulus heating parameterization of Lau and Peng we have generated an eastward propagating mode which resemblances well the observed 30-50 day mode. The model generated wave has a period of 25 days and a two layer structure in the vertical. The structure of the wave is that of a composite of Kelvin and Rossby waves and it moves eastwards.

(*ii*) When moisture is introduced in a linear two level model we obtain slow eastward moving Kelvin waves and westward moving Rossby waves. The inertia gravity waves also slow down.

(*iii*) In both the nonlinear model and the linear study as we increase the moisture availability factor the eastward moving wave slows down. The phase speed is smaller and hence the period is longer in the non-linear model. For a given drag at some critical moisture availability factor the wave becomes stationary. In the linear model both eastward moving Kelvin waves and the westward moving Rossby waves slow down with increasing moisture and become stationary for $m=0.9$ (for all values of drag). In the nonlinear model the composite wave slows down when moisture increases. The critical moisture for which the wave becomes stationary appears to depend upon the drag. When the moisture is increased further we get westward movement.

Acknowledgement

The authors wish to thank Dr. W.K.M. Lau for many helpful discussions.

References

Alexander, G., Keshavamurty, R.N., De, U.S., Chellapa, R., Das, S.K. and Pillai, P.V., 1978, Fluctuations of monsoon activity, *Indian J. Met. Hydrol. Geophys.*, **29**, 76-87.

Bourke, W., 1974, A multi-level spectral model I. Formulations and Hemispheric Integrations, *Mon. Weath. Rev.*, **102**, 687-701.

Chang, C.P. and Lim, H., 1988, Kelvin wave-CISK : A possible mechanism for the 30-50 day oscillation, *J. Atmos. Sci.*, **45**, 1709-1720.

Chao, W.C., 1987, On the origin of the tropical intraseasonal oscillation, *J. Atmos. Sci.*, **44**, 1940-1949.

Dakshinamurti, J. and Keshavamurty, R.N., 1976, On oscillation of period around one month in the Indian summer monsoon, *Indian J. Met. Hydrol. Geophys.*, **27**, 201-208.

Hendon, H.H., 1988, A simple model of the 40-50 day oscillation, *J. Atmos. Sci.*, **45**, 569-584.

Kasture S.V. and Keshavamurty, R.N., 1987, Some aspects of the 30-50 day oscillation, *Proc. Indian Acad. Sci. (Earth & Planet Sci.)* **96**, 49-58.

Keshavamurty, R.N., Kasture, S.V. and Krishnakumar, V., 1986, 30-50 day oscillation of the monsoon—A new Theory, *Beiter, Phys. Atmos.*, **59**, 443-454.

Knutson, T.R., Weickmann, K.M. and Kutzbach, J.E., 1980, Global scale intraseasonal oscillations of outgoing long wave radiation and 250 mb zonal wind during the northern hemisphere summer, *Mon. Weath. Rev.*, **114**, 605-623.

Krishnamurti, T.N. and Subrahmanyam, D., 1982, The 30-50 day mode at 850 mb during MONEX, *J. Atmos. Sci.*, **39**, 2088-2095.

Krishnamurti, T.N., Jayakumar, P.K., Sheng, J., Surgi, N. and Kumar, A., 1985, Divergent circulations on the 30-50 day time scale, *J. Atmos. Sci.*, **42**, 364-375.

Lau, K.M. and Chan, P.H., 1983 (a), Short term climate variability and atmospheric teleconnection as inferred from outgoing long wave radiation Part I : Simultaneous relationships, *J. Atmos. Sci.*, **40**, 2735-2750.

Lau, K.M. and Chan, P.H., 1983 (b), Short term climate variability and atmospheric teleconnection as inferred from outgoing long wave radiation. Part II : Lagged correlations, *J. Atmos. Sci.*, **40**, 2751-2767.

Lau, K.M. and Chan, P.H., 1985, Aspects of the 40-50 day oscillation during northern winter from outgoing long wave radiation, *Mon. Weath. Rev.*, **113**, 1889-1909.

Lau, K.M. and Chan, P.H., 1986(a), Aspects of the 40-50 day oscillation during the northern summer as inferred from outgoing long wave radiation, *Mon. Weath, Rev.*, **114**, 1354-1369.

Lau, K.M. and Peng, L., 1987, Origin of low frequency '(Intra-seasonal) oscillations in the Tropical Atmosphere Part I : Basic Theory, *J. Atmos. Sci.*, **44**, 950-972.

Lorenc, A.C., 1984, The exclusion of planetary scale 200 mb divergent flow during the FGGE year, *Quart. J.R. Met. Soc.*, **110**, 427-441.

Madden, R.A. and Julian, P.R., 1971, Detection of a 40-50 day oscillation in the zonal wind in the tropical pacific, *J. Atmos. Sci.*, **28**, 702-708.

Mohanty, U.C. and Das, S., 1986, On the structure of the atmosphere during suppressed and active period of convection over the Bay of Bengal, *Proc. Indian Nat. Sci. Acad.*, **52**, 625-640.

Murakami, T., Nakawa and Jin, H.H., 1983, 40-50 day oscillation during the 1979 Northern Hemisphere, Summer Tech. Report No. UMMET 83-02 Department of Meteorology, Univ. of Hawaii, Honolulu, Hawaii.

Sikka, D.R. and Gadgil, S., 1980, On the maximum cloud zone and the ITCZ over India longitude during southwest monsoon, *Mon. Weath. Rev.*, **108**, 1840-1853.

Weickmann, K.M., Lussky, G.R. and Kutzbach, J.E., 1975, Intraseasonal (30-50 day) fluctuations of the outgoing long wave radiation 250 mb stream function during northern winter, *Mon. Weath. Rev.*, **113**, 941-961.

Yasunari, T., 1979, Cloudiness fluctuations associated with the northern hemisphere summer monsoon, *J. met. Soc. Japan*, **57**, 227-242.

Yasunari, T., 1980, A quasi-stationary appearance of the 30-50 day period in the cloudiness fluctuations during the summer monsoon over India, *J. met. Soc. Japan*, **58**, 225-229.